Tetrahedron: *Asymmetry* 26 (2015) 1043–1049

Contents lists available at ScienceDirect

Tetrahedron: *Asymmetry*

journal homepage: www.elsevier.com/locate/tetasy

Vibrational and electronic circular dichroism studies on the axially chiral pyridine-*N*-oxide: *trans*-2,6-di-*ortho*-tolyl-3,4,5-trimethylpyridine-*N*-oxide

Florina Teodorescu [a], Simona Nica [a], Cornelia Uncuta [a], Emeric Bartha [a], Petru Ivan Filip [a], Nicolas Vanthuyne [b], Christian Roussel [b], Attila Mándi [c], László Tóth [c], Tibor Kurtán [c], Jean-Valère Naubron [d,*], Isabela-Costinela Man [a,*]

[a] *Institute of Organic Chemistry 'C. D. Nenitzescu' of Romanian Academy, Spl. Independentei, 202B, PO Box 35-108, 060023 Bucharest, Romania*
[b] *Aix-Marseille Université, UMR ISM2: Chirosciences, Marseille, France*
[c] *Department of Organic Chemistry, University of Debrecen, Egyetem ter 1, 4010 Debrecen, P.O.B. 20, Hungary*
[d] *Aix-Marseille Université, Spectropole, FR1739 Marseille, France*

ARTICLE INFO

Article history:
Received 19 June 2015
Accepted 13 August 2015
Available online 29 August 2015

It is a privilege to dedicate this account to the memory of Cornelia Uncuta (1944–2012), from whose early work on pyridine class much has followed

ABSTRACT

The absolute configuration of the resolved axially chiral pyridine-*N*-oxide derivative, (±)-*trans*-2,6-di-*ortho*-tolyl-3,4,5-trimethylpyridine-*N*-oxide, has been determined by VCD and ECD analyses supported by TD-DFT calculations carried out at different levels of theory. DFT calculations confirmed that in spite of the two biaryl axes, the compound is conformationally less flexible and the major conformer is stabilized by two weak hydrogen bonds formed between the hydrogen of the methyl group of the tolyl moieties and the nitroxide oxygen. The experimental VCD spectra of this compound and the previously studied (±)-2,6-di-sec-butyl-4-methylpyridine-N-oxide with two stereogenic centers were compared in the frequency range 1200–1300 cm^{-1}. A (+,−,+)/(−,+,−) pattern of bands was observed in both cases. By replacing the *sec*-butyl moieties with tolyl ones, the VCD peaks shifted toward higher frequencies and the intensities were increased.

1. Introduction

Chiral pyridine-*N*-oxides have been being studied for several years in the field of asymmetric homogeneous catalysis, as shown in recent reviews.[1–5] Typical reactions tested so far for enantioselectivity include allylations of aldehydes with polyhalosilanes,[6–21] aldol additions of trichlorosilylenol ethers to aldehydes[6,7,22] or ketones,[23,24] and epoxide ring openings[25–27] as typical tested enantioselective reactions.

The structural diversity covers pyridine-*N*-monoxides,[19,25] quinoline-*N*-oxides,[5,15,21,26] 2,2′-bis-pyridine-*N*-monoxides[11,12,14] and *N*,*N*′-dioxides,[8–10,23,24,28,29] 2,2′-bis-quinoline-*N*,*N*′-dioxides,[6,21,23] dipyridilmethane-*N*-monoxides and *N*,*N*′-dioxides,[13,30] terpyridine tri-*N*-oxides,[17] and other chiral pyridine *N*-oxides. Their stereochemical diversity is relatively rich involving axial chirality,[8,10,15,19,21,26] axial plus central chirality,[12,14,23,24,28] multicentered chirality originating in monoterpene units,[11,13,14,30] and planar[25] and helical chirality.[27] Since each type of chirality has its inherent structural feature, a variety of procedures has been used for establishing the absolute configuration of enantiopure pyridine-*N*-oxides. Reliable configurational assignments have been obtained by X-ray analysis of crystalline derivatives with optically active reagents (*R*)- and (*S*)-BINOL.[31–33] The increase in the number, as well as in the structural and stereochemical diversity of chiral pyridine-*N*-oxides calls for a general and reliable method for configurational assignment. Over the last few decades, the VCD technique has proven to be a powerful tool for assigning the absolute configuration and predominant conformations in solution for compounds with various types of chirality.[34–36] In our previous study, we introduced the vibrational circular dichroism (VCD) as an efficient method for the determination of the absolute configuration of chiral pyridine-*N*-oxides.[37] The studied molecule, 2,6-di-*sec*-butyl-4methylpyridine-*N*-oxide, had a conformationally flexible structure possessing two stereogenic centers. In the present example, we succeeded in assigning the (+)-(a*S*,a*S*)/(−)-(a*R*,a*R*) enantiomers of the conformationally rigid C_2-symmetrical *trans*-2,6-di-*ortho*-tolyl-3,4,5-trimethylpyridine-*N*-oxide possessing two identical chiral axes, by VCD measurements combined with DFT calculations. Since it is recommended to apply more than one chiroptical method for the unambiguous stereochemical study

* Corresponding authors. Tel.: +33 0491 28 8641 (J.-V.N); tel.: +40 21 316 79 00; fax: +40 21 312 16 01 (I.-C.M.).
E-mail addresses: jean-valere.naubron@univ-amu.fr (J.-V. Naubron), isabela.man@cco.ro (I.-C. Man).

http://dx.doi.org/10.1016/j.tetasy.2015.08.006
0957-4166/

of any given molecule,[38] we also verified the absolute configuration by electronic circular dichroism (ECD) spectroscopy and TD-DFT calculations.

2. Results and discussion

2.1. Preparation and resolution of *trans*-1

The pyridine-*N*-oxide **1** was selected for VCD and ECD studies. A similar study was previously reported by our research group for a flexible pyridine-*N*-oxide compound with two stereogenic centers but only the VCD study was performed.[39] Due to the two chiral axes and symmetry, compound **1** has three stereoisomers; the achiral (C_S) *cis*-isomer with an (a*S*,a*R*)-configuration and the (a*S*, a*S*)- and (a*R*,a*R*)-enantiomers of the chiral (C_2) *trans*-isomer (the *cis*, *trans* descriptors are related to the position of methyl groups of *o*-tolyl rings: on the same side or on opposite sides of the heterocycle-see Fig. 1 for *trans* isomers). The pyridine-*N*-oxide moiety together with the two aryl chromophores have different arrangements in the (a*S*,a*S*) and (a*R*,a*R*) enantiomers, which allows them to be distinguished by VCD and ECD.

The synthesis of pyridine-*N*-oxide **1** was based on the reaction of pyrylium salts with hydroxylamine[40] and is shown in Scheme 1. Dehydration of 3-methyl-pentan-3-ol afforded alkenes **3** and **4**. Diacylation of this mixture with *o*-tolyl chloride in the presence of aluminum chloride as catalyst[41] gave the isomeric pyrylium salts **5** and **6** in an 85:15 ratio. Treatment with hydroxylamine gave the pyridine-*N*-oxides **1** and **7**, respectively, along with small amounts of pyrylium salt anhydrobase **8**.

The ^{1}H NMR spectrum of the crude reaction mixture showed that compound **1** was obtained as two diastereoisomers in a 40:60 ratio. Chiral HPLC analysis of the mixture with UV/polarimetric detection identified the major diastereomer as chiral *trans* and the minor one as achiral *cis*. By successive column and thin-layer chromatography of this mixture, the target compounds *rac*-*trans*-**1** and *cis*-**1** were obtained with up to 90–92% diastereomeric purity.

Initial attempts to resolve racemic *trans*-**1** by fractional crystallization of diastereomeric salts with (*R*)-(−)-1,1′-binaphthyl-2, 2′-diyl hydrogen phosphate or by complexation with (+)-(*R*)-2,2′-binaphthol were unsuccessful. The resolution succeeded by HPLC using chiral stationary phase based upon cellulose tris(3,5-dichlorophenylcarbamate)polymer immobilized on silica using proprietary techniques, providing enantiopure samples of (+)- and (−)-**1** for VCD and ECD measurements.

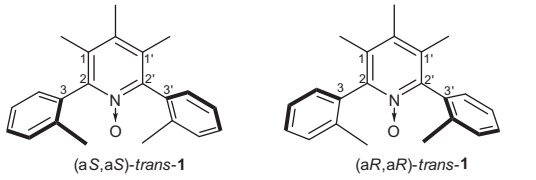

Figure 1. Structures of the (a*S*,a*S*)- and (a*R*,a*R*)-enantiomers of *trans*-2,6-di-*ortho*-tolyl-3,4,5-trimethylpyridine-*N*-oxide **1**.

2.2. Intramolecular hydrogen bonding

The conformational analysis of (a*R*,a*R*)-**1** (arbitrarily chosen) at the AM1 semiempirical level using potential energy surfaces scan method as implemented in Ampac, showed that it is a conformationally rigid molecule and that it has only one conformer as shown in Figure 1. Reoptimization of the AM1 geometry was performed at DFT level using a series of functionals (B3LYP, B3PW91, CAMB3LYP) and basis sets (6-311++Gdp, TZVP, cc-pVDZ) including the implicit polarizable continuum model (PCM) for CCl_4 as the solvent that uses the integral equation formalism variant (IEF) as implemented in Gaussian09.[42]

Similarly to the previously studied 2,6-di-*sec*-butyl-4-methyl-pyridine-*N*-oxide **9** derivative,[37] the two intramolecular hydrogen bonds formed between the hydrogen of the methyl groups and the nitroxide oxygen govern the relative orientations of the tolyl moieties. The length of the D(H···O) intramolecular hydrogen bond, the ∠(C—H···O) angle and the stabilization energy $E^{(2)}$ vary with the applied functionals and basis sets (see Table 1). With the exception of the B3LYP/TZVP method, all of the D(H···O) and D(O...H′) values are smaller than the van der Waals separation value of 2.72 Å, while the C–H···O angles are higher than 100°. The NBO analysis carried out at B3LYP/B3PW91/CAMB3LYP functionals and TZVP/cc-ppVDZ basis sets indicates very weak intramolecular donor–acceptor orbital interactions corresponding to the hydrogen–oxygen intramolecular contact, between the LP(3)O→BD*(1)C–H/BD*(1)C′–H′. In Figure 2 the overlapping between the oxygen lone pair orbital LP(3) and the antibonding orbitals of C–H bonds is visualized. The two geometric criteria together with the values of stabilization energies confirm the formation of two weak C–H···O intramolecular hydrogen bonds.

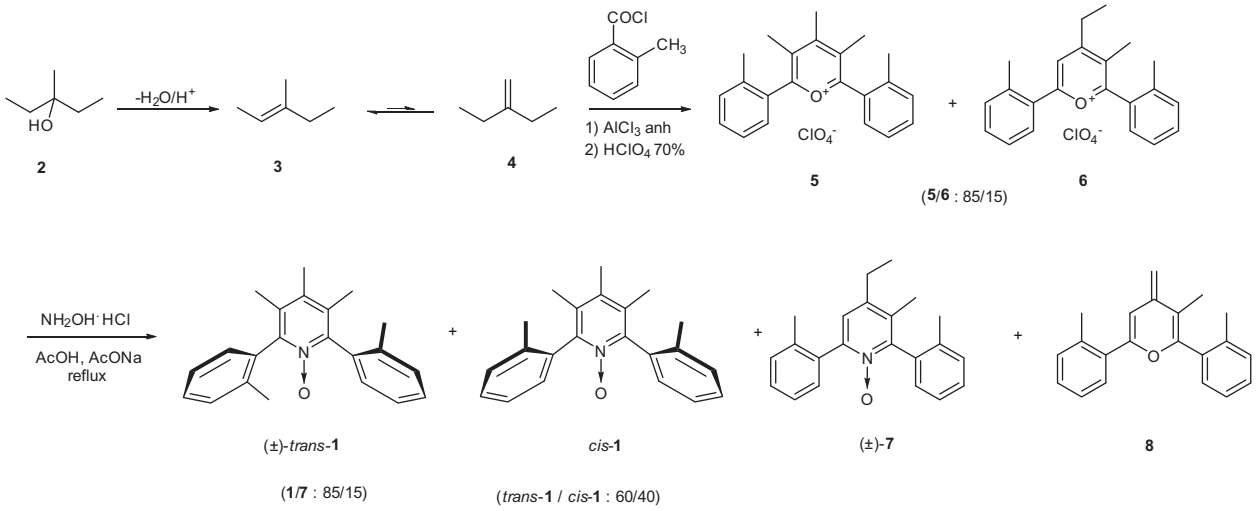

Scheme 1.

Table 1
Non-bonded $D_{(H\cdots O)}$ interatomic distances and $\sphericalangle$(C—H···O) angles, as obtained after geometry optimization using B3LYP, B3PW91, CAMB3LYP functionals and 6-311++Gdp, TZVP and cc-PVDZ basis sets. Second order perturbation theory analysis of the Fock matrix in NBO analysis for intramolecular hydrogen bond. Stabilization energy for electron transfer from LP(3)O to antibonding orbitals of C–H bonds

Functional/basis set	$D_{(H\cdots O)}$ (Å)	$D_{(O\cdots H')}$ (Å)	$\sphericalangle$(C—H···O) (°)	$\sphericalangle$(O···H′–C′) (°)	$E^{(2)}_{(LP(3)O\rightarrow BD^*(1)C-H)}$ kcal/mol	$E^{(2)}_{(LP(3)O\rightarrow BD(1)^*C'-H')}$ kcal/mol
B3LYP/6-311++Gdp	2.60	2.63	119.17	119.05	—	—
B3LYP/TZVP	2.64	2.61	121.95	118	0.4	0.4
B3LYP/cc-PVDZ	2.40	2.41	122.19	121.99	0.7	0.7
B3PW91/6-311++Gdp	2.57	2.59	119.37	119.46	—	—
B3PW91/TZVP	2.51	2.55	118.72	118.54	0.4	0.4
B3PW91/cc-PVDZ	2.40	2.41	122.37	122.12	0.4	0.4
CAMB3LYP/6-311++Gdp	2.52	2.54	120.94	120.88	—	—
CAMB3LYP/TZVP	2.52	2.55	120.67	120.53	0.8	0.7
CAMB3LYP/cc-PVDZ	2.34	2.35	123.58	123.42	1.6	1.5

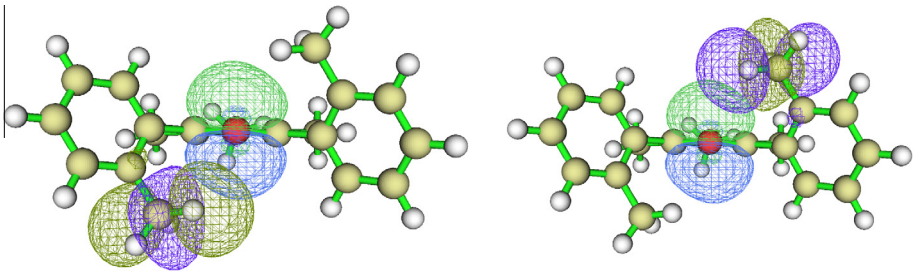

Figure 2. Interaction between the NLMO oxygen lone pair orbital LP3 (shown in light blue and green) and the corresponding C–H (left) and C′–H′ (right) σ_* empty orbitals (shown in dark blue and green). The orbitals were visualized with the aid of multiwfn software.

Concerning the most important stabilization energies within the molecule, they are given by the resonance as in the case of 2,6-di-*sec*-butyl-4-methylpyridine-*N*-oxide **9**.[37] Therefore the interaction energy calculated at B3PW91/TZVP level (the same level used for calculations of the flexible conformers of 2,6-di-*sec*-butyl-4-methylpyridine-*N*-oxide **9**) for charge transfer from LP(3) O to the antibonding acceptor π_*(N–C_2') is 52.5 kcal/mol and is higher than in the case of conformers of **9**, which is in the range 35–45 kcal/mol. As in the case of a flexible molecule, this π_*(N–C_2') NBO further conjugate with π_*(C_2'–C_1') resulting in the strongest stabilization energy of 63.3 kcal/mol. Besides the conjugation inside the pyridine ring, it conjugates as well with the π_*(C_3'–$C_{x/y}'$) antibonding orbitals of the tolyl ring but the energy values are much lower compared with the stabilization energies shown for the conjugation inside the pyridine ring.

2.3. Experimental IR and VCD spectra analysis: comparison of the VCD spectra of (+)- and (−)-*trans*-1 with (+)- and (−)-2,6-di-*sec*-butyl-4-methylpyridine-*N*-oxide. Absolute configuration determination of (+)- and (−)-*trans*-1 by VCD analysis

The experimental IR and VCD spectra of enantiomers were recorded in CCl_4 solution at a concentration of 0.06 mol L^{-1}, in the frequency range of 1800–1000 cm^{-1}. To minimize the artifacts, the baseline of the VCD spectra was corrected with the VCDs of the enantiomers [(+)-**1** + (−)-**1**]/2. Figure 3a shows the IR spectrum and the corrected VCD spectra of (+)- and (−)-*trans*-**1**.

In order to explore the important part of the VCD spectra, we divided the experimental spectra into three regions. In the first region, bands derive from the ring stretching modes, deformations, asymmetric and symmetric bending vibrations of the methyl groups. The most intense VCD band in this region is at ν = 1464 cm^{-1} and is due to methyl asymmetric C–H bending.

In the second region, three VCD bands arise from a (+,−,+)/(−,+,−) triplet of modes near 1330, 1296 and 1284 cm^{-1} representing the C–H bending motion of the aryl moieties along mutually orthogonal directions and the N→O stretching vibrations. The same triplet of modes appear in the spectrum of the previously similar studied molecule 2,6-di-*sec*-butyl-4 methylpyridine-*N*-oxide **9** (see the comparison in Fig. 3b), which is a flexible *N*-oxide derivative with two stereogenic centers. For *trans*-**1**, the bands are shifted toward higher frequencies and are much more intense. The intense triplet mode observed and calculated (Fig. 3b) for these vibrational modes might be a consequence of the mixing between the breathing mode of the nitroxide aryl moiety and the two aryl groups maintained in a particular position by weak hydrogen bonds.

The third region contains a number of low intensity vibrational bands related to vibrational motions of the C–H of methyl group and of C–C and C–H bonds of the rings.

Simulations of the IR and VCD spectra of (a*R*,a*R*)-*trans*-**1** using Lorentzian bandshapes (γ = 4.0 cm^{-1}) are shown in Figure 3, together with the corresponding experimental spectra in the frequency range 1700–1000 cm^{-1}. The IR and VCD spectra were predicted using the B3LYP, B3PW91 and CAMB3LYP functionals and the 6-311Gdp, 6-311++Gdp, TZVP and cc-PVDZ basis sets. The shape of both IR and VCD spectra calculated with 6-311Gdp and 6-311++Gdp is the same. For this reason, we did not calculate the equivalent case for cc-pVDZ basis set with diffuse functions, the aug-cc-pVDZ.

The vibrational frequencies, the IR and VCD intensities were constructed from calculated dipole and rotational strengths assuming Lorentzian band shape with half width at half maximum of 4 cm^{-1}.

The best agreement between the experimental and calculated IR and VCD spectra in the entire range of frequencies was achieved with CAMB3LYP/TZVP and 6-311++Gdp/6-311Gdp (not shown for 6-311Gdp) methods (see Fig. 4). Therefore the assignment of the experimental spectra is based on these combinations and indicates that (−)-*trans*-**1** has an (a*R*,a*R*)-absolute configuration. Satisfactory

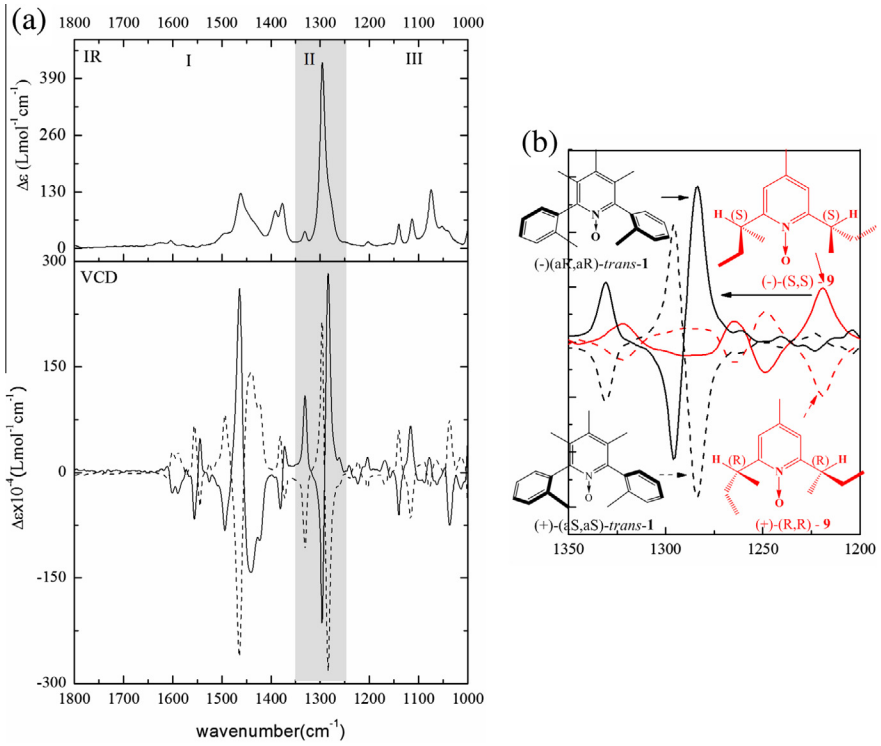

Figure 3. (a) Experimental IR and VCD spectra of (+)- and (−)-*trans*-**1** in CCl_4 solution (0.06 M, 500 μm path, 4 cm^{-1} resolution). (b) Experimental VCD spectra in the frequency region ν = 1350–1200 and represent the comparison between the (+,−,+)/(−,+,−) triplet of modes encountered in both VCD spectra of (+)- and (−)-*trans*-**1** and (+)- and (−)-2,6-di*sec*-butyl-4-methylpyridine-*N*-oxide.

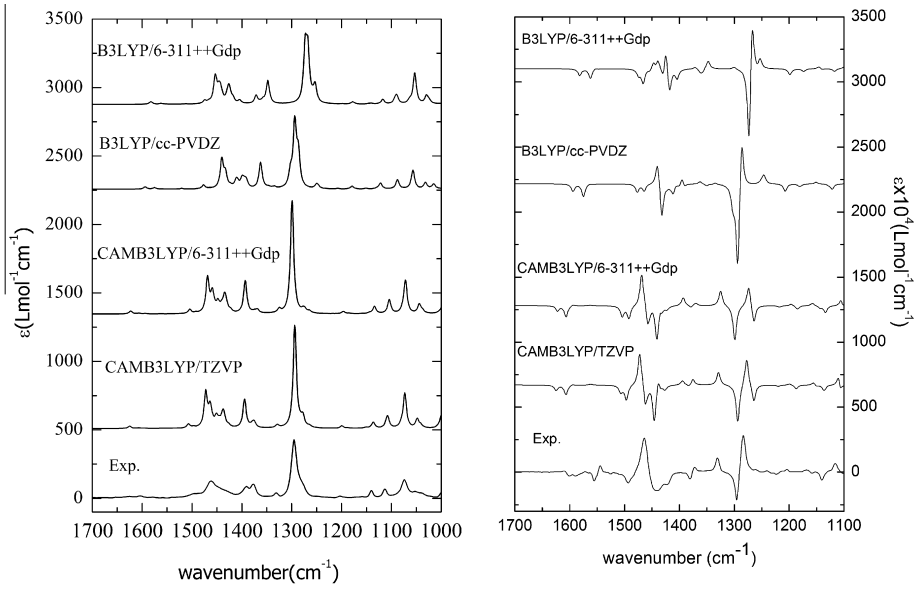

Figure 4. Comparison of the CAMB3LYP/TZVP, CAMB3LYP/6-311++Gdp, B3LYP/cc-PVDZ, B3LYP/6-311++Gdp spectra of (a*R*,a*R*)-*trans*-**1** to the experimental IR and VCD spectra of (−)-*trans*-**1**.

agreements were also obtained with B3LYP/cc-PVDZ and B3LYP/6-311++Gdp (6-311Gdp) (Fig. 4) indicating the same (a*R*,a*R*)-absolute configuration of the (−)-*trans*-**1** enantiomer.

2.4. Absolute configuration of (+)- and (−)-*trans*-1 by ECD analysis

The online HPLC-ECD spectra of (+)- and (−)-*trans*-**1** were recorded upon separation of the enantiomers on a Chiralcel OD column with hexane/2-propanol 90:10 as an eluent, which showed a mirror image ECD curves. The first eluting enantiomer was identified as the (−)-*trans*-**1** enantiomer. The ECD spectra of the separated enantiomers were also recorded in acetonitrile.

The AM1 structure of (a*R*,a*R*)-*trans*-**1** was reoptimized at the B3LYP/6-31Gd level of theory. Then ECD calculations were carried out with B3LYP, BH&HLYP and CAM-B3LYP functionals and TZVP basis set. All three applied levels for the ECD calculations gave good agreement with the spectra of (−)-*trans*-**1**, but CAM-B3LYP represent somewhat better the experimental spectrum in the 200–225 nm range (see Fig. 5). Thereby the ECD calculations

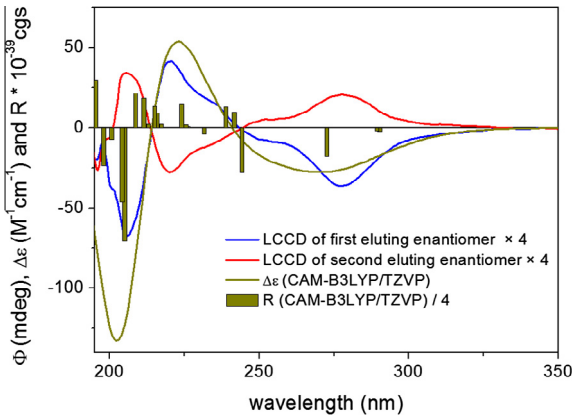

Figure 5. Experimental HPLC-ECD spectra of (−)-(a*R*,a*R*)-**1** (blue) and (+)-(a*S*,a*S*)-**1** (red) compared with the TDDFT computed ECD spectra (CAM-B3LYP/TZVP, olive) for the solution conformer of (a*R*,a*R*)-**1**; vertical bars represent rotational strengths calculated at the CAM-B3LYP/TZVP level.

verified the results obtained with VCD and indicated that the absolute configuration of (−)-*trans*-**1** is (a*R*,a*R*).

3. Conclusion

This study is a continuation of our previously related VCD study of pyridine-*N*-oxide compounds. A similar compound to (±)-2,6-di-*sec*-butyl-4-methylpyridine-*N*-oxide was synthesized, in which the *sec*-butyl moieties were replaced with tolyl groups and the methyl groups were attached to the pyridine ring. Major molecule structural changes took place either in the type of chirality or in the flexibility of the molecule. The newly resolved enantiomers (−)- and (+)-*trans*-2,6-di-*ortho*-tolyl-3,4,5-trimethylpyridine-*N*-oxide are biaxially chiral and are rigid molecules that imply a unique conformer. The synthesis and the resolution steps of the enantiomers were detailed. The unique conformer was confirmed by DFT calculations and it was shown that the conformation of the enantiomer is given by the two simultaneous intramolecular hydrogen bonds that form between the hydrogen of the methyl groups belonging to the tolyl moieties attached to the pyridine-*N*-oxide ring and the nitroxide oxygen. The experimental VCD and ECD studies combined with DFT and TD-DFT theoretical calculations were performed at various levels of theories and showed that (−)-*trans*-**1** had an (a*R*,a*R*)-absolute configuration.

A comparison of the experimental VCD spectra of (−)- and (+)-2,6-di-*sec*-butyl-4-methylpyridine-*N*-oxide and of (−)- and (+)-*trans*-2,6-di-*ortho*-tolyl-3,4,5-trimethylpyridine-*N*-oxide in the frequency range 1200–1300 cm^{-1}, revealed that both have a (+,−,+)/(−,+,−) triplet and when the *sec*-butyl moieties are replaced with tolyl moieties, the peaks shift toward higher frequencies and have higher intensities. The existence of this triplet could in the future ease the VCD spectra interpretation of the pyridine like compounds. Some supplementary data will be acquired in the future so as to increase the database and to establish if possible a correlation between the peak signs and a particular characteristic of the pyridine compounds such as to be able to extrapolate the finding to the entire class of optically active pyridine derivatives.

4. Experimental

4.1. Instrumentation

4.1.1. Synthesis and enantiomeric resolution

The NMR spectra were recorded with Varian Gemini 300 BB instrument, operating at 300 MHz for ^1H NMR and at 75 MHz for ^{13}C NMR, in $CDCl_3$ solution at room temperature. The chemical shift (δ) values are given in ppm from internal TMS, and the coupling constants *J* are in Hz.

Analytical TLC was performed with silica gel F_{254} (Merck) on aluminum strips (10 cm length). The elemental analysis was performed with an ECS 4010 COSTECH instrument. For column chromatography and preparative TLC, silica gel 60 (Merck) and silica gel F_{254} plates 20 × 20 cm (Merck) were used. The elution solvents used for chromatography were diethylether and petrol, boiling range 40–67 °C.

The chiral HPLC analyses were performed on a Chiralpak IC column (5 μm, 150 × 4.6 mm, hexane/ethanol 50:50 eluents, 1 mL min^{-1} flow rate) on a unit composed of Merck D-7000 system manager, Merck-Lachrom L-7100 pump, Merck-Lachrom L-7200 autosampler, Merck-Lachrom L-7360 oven, Merck-Lachrom L-7400 UV-detector and Jasco OR-1590 polarimeter. Retention times *Rt* in minutes, retention factors $k_i = (Rt_i - Rt_0)/Rt_0$ and enantioselectivity factor $\alpha = k_2/k_1$ are given. Rt_0 was determined by injection of tri-*t*-butyl benzene.

4.1.2. IR and VCD measurements

IR and VCD spectra were recorded on a Bruker PMA 50 accessory coupled to a Vertex70 Fourier transform infrared spectrometer. A photoelastic modulator (Hinds PEM 90) set at l/4 retardation was used to modulate the handedness of the circular polarized light at 50 kHz. Demodulation was performed by a lock-in amplifier (SR830 DSP). An optical low-pass filter (<1800 cm^{-1}) before the photoelastic modulator was used to enhance the signal/noise ratio. A transmission cell equipped with CaF_2 windows and a 500 μm spacer was used and the solid samples were measured in CCl_4 at a concentration of 0.06 mol·L^{-1}. Baseline and artifact corrected VCD spectrum of one enantiomer was obtained by subtraction of the VCD spectrum of a sample of the opposite enantiomer and division by two. For the two enantiopure samples the interferogram was averaged over totally two hours in time slices of 15 min at a resolution of 4 cm^{-1}. For the infrared spectrum the cell with CCl_4 served as reference. The spectra are presented without smoothing and further data processing.

4.1.3. HPLC-ECD measurements

Chiral HPLC separation of the *trans*-**1** enantiomer were performed on a Jasco HPLC system with Chiralcel OD column (5 μm, 150 × 4.6 mm, hexane/propan-2-ol 80:20 eluents, 1 mL min^{-1} flow rate) and HPLC-ECD spectra were recorded in stopped-flow mode on a JASCO J-810 electronic circular dichroism spectropolarimeter equipped with a 10 mm HPLC flow cell. ECD ellipticity (Φ) values were not corrected for concentration. For an HPLC-ECD spectrum, three consecutive scans were recorded and averaged with 2 nm bandwidth, 1 s response, and standard sensitivity. The HPLC-ECD spectrum of the eluent recorded in the same way was used as background. The concentration of the injected sample was set so that the HT value did not exceed 500 V in the HT channel down to 210 nm.

4.2. Synthesis of pyridine-1-oxide 1 and the separation of the stereoisomers

In Scheme 1 is presented the perchlorate of 2,6-di-*o*-tolyl-3,4,5-trimethylpyrylium salt **5**. Anhydrous aluminum chloride (67.0 g, 0.5 mol) was added in portions to *o*-toluyl chloride (154.5 g, 1 mol) under stirring and with external cooling in an ice/water bath. Next, 42 g (0.5 mol) of 3-methyl-2-pentene **3** (obtained by dehydration of 3-methyl-3-pentanol with sulfuric acid and containing 15% 2-ethyl-1-butene **4**) was added dropwise, while maintaining the inner temperature under 10 °C. After stirring for 2–2.5 h at this temperature, the mixture was left overnight at room temperature, then heated for 1 h at 45–55 °C and poured still

warm over 50 mL of concentrated hydrochloric acid diluted with 200 g of ice-water. The mixture was transferred to a separation funnel and diluted with diethyl ether; the aqueous phase was separated and further extracted two times with diethyl ether. Upon the addition of 70% perchloric acid to the aqueous layer, pyrylium salt precipitated and then filtered off. Recrystallization from glacial acetic acid gave pyrylium perchlorate **5** in 25% yield (purity 85%, isomeric salt **6** as by-product). 2,6-Bis-(2-methylphenyl)-3,4,5-trimethylpyrylium perchlorate **5**: mp 212–6 °C; Anal. Calcd for $C_{22}H_{23}ClO_5$: C, 65.59; H, 5.71; Cl, 8.82. Found: C, 65.67; H, 5.85; Cl, 8.48.

2,6-Di-*o*-tolyl-3,4,5-trimethylpyridine-1-oxide **1**: to pyrylium perchlorate **5** (500 mg, 1.24 mmol) in 10 mL of glacial acetic acid was added, under magnetic stirring, hydroxylamine hydrochloride (435 mg, 6.25 mmol). The mixture was brought to boiling, then crystalline sodium acetate (2.89 g, 21.23 mmol) was added at once. We noticed that adding sodium acetate at the beginning and heating afterward led to a significant increase in the amount of the anhydrobase of the pyrylium salt, compound **8**. The mixture was heated at reflux for 30 min, then acetic acid was distilled under vacuum and cold water was added. The mixture was extracted three times with chloroform, the organic layer was neutralized with aqueous sodium dicarbonate and dried over sodium sulfate. Evaporation of the solvent gave an oil (519 mg). The crude product was purified by column chromatography on silica gel: anhydrobase **8** was separated with 10% (v) diethylether/petrol, then a mixture of pyridine-1-oxides **1** and **7** was eluted with diethylether (342 mg, 70% yields).

The mixture of **1** and **7** was further subjected to preparative thin layer chromatography, eluting three times with 50% (v) diethylether/petrol and two times with diethylether. The spread area was fractioned into four distinct zones, which after elution with diethylether and evaporation of the solvent gave (in decreasing R_f order): **7** (33 mg); *trans*-**1** (92% diastereomeric purity, 154 mg); an intermediate fraction consisting of *trans*- and *cis*-**1** in an almost 1:1 ratio (64 mg) and *cis*-**1** (90% diastereomeric purity, 54 mg).

4.3. Computational details

The conformational analysis of (a*R*,a*R*)-*trans*-**1** was carried out primarily at a lower level of theory. This involved exploring the entire conformational energy surface of the molecule and carrying out semiempirical AM1 calculations with the PES scan technique as both implemented in the package Ampac.

Upon further geometry optimization, the vibrational frequencies, absorption, and VCD intensities were calculated by Gaussian 09 program. Calculations of the optimized geometry of the unique conformer of (a*R*,a*R*)-*trans*-**1** were performed at the density functional theory level using B3LYP, B3PW91, CAMB3LYP functionals and 6-311Gdp, 6-311++Gdp, TZVP and cc-PVDZ basis sets. Vibrational frequencies, IR and VCD intensities were calculated at the same levels of theory, using the magnetic field perturbation method with gauge-invariant atomic orbitals. The implicit solvent effect (CCl_4) was taken into consideration when using the polarizable continuum model with integral equation formalism variant (IEFPCM). For the sake of comparison to the experiment, the calculated frequencies were scaled by 0.965 and the calculated intensities were converted to Lorenzian bands with a half width of 4 cm^{-1}. By the use of the second-order bond antibond (donor–acceptor) NBO energetic analysis, insight into the intra-molecular hydrogen bonding was obtained. The $E^{(2)}$ stabilization energies were calculated by natural bond orbital (NBO) analysis as implemented in Gaussian using the same functionals and basis sets.

Reoptimization for the ECD calculations performed at B3LYP/6-31G(d) level of theory in vacuo and TDDFT calculations using various functionals (B3LYP, BH&HLYP, CAM-B3LYP) and TZVP basis set were performed by the Gaussian 09 package. ECD spectra were generated as the sum of Gaussians with 3000 cm^{-1} half height width (corresponding to ca. 15 nm at 225 nm), using dipole-velocity computed rotational strengths.[43] *cis*- and *trans*-2,6-Bis-(2-methylphenyl)-3,4,5-trimethylpyridine-1-oxide **1**: Anal. Calcd for $C_{22}H_{23}NO$: C, 83.28; H, 7.26; N, 4.42. Found: C, 82.97; H, 7.59; N, 4.27. *cis*-**1**, ^{1}H NMR: 2.03 (6H, s), 2.11 (6H, s), 2.29 (3H, s), 7.10–7.30 (8H, m). (±)-*trans*-**1**, ^{1}H NMR: 2.03 (6H, s), 2.12 (6H, s), 2.29 (3H, s), 7.10–7.30 (8H, m). Chiral HPLC analysis: Chiralpak IC (250 × 4.6 mm), hexane/ethanol 50:50, 1 mL min^{-1}, 25 °C, UV detection at 254 nm and polarimeter, $R_t(+) = 8.06$, $R_t(-) = 10.23$, $k(+) = 1.06$, $k(-) = 2.3$, $\alpha = 1.44$. Chiralcel OD (250 × 4.6 mm) hexane/2-propanol 90:10, 1 mL min^{-1}, 25 °C, UV, OR and ECD detection at 280 nm $R_t(-) = 10.33$, $R_t(+) = 16.50$.

(+)-(aS,aS)-*trans*-**1** $[\alpha]_D^{25} = +167.6$, ECD (MeCN, λ[nm] ($\Delta\varepsilon$), $c = 2.45 \times 10^{-4}$ M): 301sh (7.9), 278 (28.8), 242 (16.9), 220 (−65.5), 205 (67.8), 194 (−23.1).

(−)-(aR,aR)-*trans*-**1** $[\alpha]_D^{25} = -171.6$, ECD (MeCN, λ[nm] ($\Delta\varepsilon$), $c = 2.81 \times 10^{-4}$ M): 302sh (−9.4), 278 (−37.2), 242 (−23.6), 220 (86.2), 205 (−90.3), 194 (25.3).

2,6-Bis(2-methylphenyl)-4-ethyl-3-methylpyridine-1-oxide, **7**, ^{1}H NMR: 1.30 (3H, t, $J = 7.4$), 2.01 (3H, s), 2.14 (3H, s), 2.26 (3H, s), 2.69 (2H, quartet, $J = 7.5$), 7.16–7.31 (9H, m).

2,6-Bis(2-methylphenyl)-3,5-dimethyl-4-methylene-4*H*-pyran, **7**, ^{1}H NMR: 1.73 (6H, s), 2.33 (6H, s), 4.50 (2H,s), 7.18–7.32 (8H, m).

Acknowledgements

F.T., I.C.M., P.I.F. acknowledge the financial support: PCCA Contract 105/2014, GreenTech, Executive Agency for Higher Education, Research, Development and Innovation (UEFISCDI); T.K. and A.M. thank the Hungarian National Research Foundation (OTKA K105871) for financial support.

References

1. Nakajima, M. J. *Synth. Org. Chem. Jpn.* **2003**, *61*, 1081.
2. Malkov, A. V.; Kocovsky, P. *Curr. Org. Chem.* **2003**, *7*, 1737.
3. Chelucci, G.; Murineddu, G.; Pinna, G. A. *Tetrahedron: Asymmetry* **2004**, *15*, 1373.
4. Malkov, A. V.; Kocovsky, P. *Eur. J. Org. Chem.* **2007**, 29.
5. Denmark, S. E.; Beutner, G. L. *Angew. Chem., Int. Ed.* **2008**, *47*, 1560.
6. Nakajima, N.; Saito, M.; Shiro, M.; Hashimoto, S. *J. Am. Chem. Soc.* **1998**, *120*, 6419.
7. Nakajima, M. *Chem. Pharm. Bull.* **2000**, *48*, 306.
8. Shimada, T.; Kina, A.; Ikeda, S.; Hayashi, T. *Org. Lett.* **2002**, *4*, 2799.
9. Shimada, T. *J. Org. Chem.* **2003**, *68*, 6329.
10. Kina, A.; Shimada, T.; Hayashi, T. *Adv. Synth. Catal.* **2004**, *346*, 1169.
11. Malkov, A. V.; Orsini, M.; Pernazza, D.; Muir, K. W.; Langer, V.; Meghani, P.; Kocovsky, P. *Org. Lett.* **2002**, *4*, 1047.
12. Malkov, A. V.; Bell, M.; Orsini, M.; Pernazza, D.; Massa, V.; Herrmann, P.; Meghani, P.; Kocovsky, P. *J. Org. Chem.* **2003**, *68*, 9659.
13. Chelucci, G.; Belmonte, N.; Benaglia, M.; Pignataro, L. *Tetrahedron Lett.* **2007**, *48*, 4037.
14. Malkov, A. V.; Bell, M.; Castelluzo, F.; Kocovsky, P. *Org. Lett.* **2005**, *7*, 3219.
15. Malkov, A. V.; Dufkova, L.; Farrugia, L. *Angew. Chem., Int. Ed.* **2003**, *42*, 3674.
16. Pignataro, L.; Benaglia, M.; Annunziata, R.; Cinquini, M.; Cozzi, F. *J. Org. Chem.* **2006**, *71*, 1458.
17. Wong, W.-L.; Lee, C.-S.; Leung, H.-K.; Kwong, H.-L. *Org. Biomol. Chem.* **2004**, *2*, 1967.
18. Charmant, J. P.; Hunt, N. J.; Lloyd-Jones, G. C.; Nowak, T. *Collect. Czech. Chem. Commun.* **2003**, *68*, 865.
19. Pignataro, L.; Benaglia, M.; Cinquini, M.; Cozzi, F.; Celentano, G. *Chirality* **2005**, *17*, 396.
20. Hrdina, R.; Kadlcikova, A.; Valterova, I.; Hodacova, J.; Kotora, M. *Tetrahedron: Asymmetry* **2006**, *17*, 3185.
21. Malkov, A. V.; Westwater, M.-M.; Gutnov, A.; Ramirez-Lopez, P.; Friscourt, F.; Kadlcikova, A.; Hodacova, J.; Rankovic, Z.; Kotora, M.; Kocovsky, P. *Tetrahedron* **2008**, *64*, 11335.
22. Nakajima, M.; Yokota, T.; Saito, M.; Hashimoto, S. *Tetrahedron Lett.* **2004**, *45*, 61.
23. Denmark, S. E.; Fan, Y. *J. Am. Chem. Soc.* **2002**, *124*, 4233.
24. Denmark, S. E.; Fan, Y.; Eastgate, M. D. *J. Org. Chem.* **2005**, *70*, 5235.
25. Tao, B.; Lo, M. M.-C.; Fu, G. C. *J. Am. Chem. Soc.* **2001**, *123*, 353.
26. Nakajima, M.; Saito, M.; Uemura, M.; Hashimoto, S. *Tetrahedron Lett.* **2002**, *43*, 8827.

27. Chen, J.; Takenaka, N. *Chem. Eur. J.* **2009**, *15*, 7268.
28. Denmark, S. E.; Fan, Y. *Tetrahedron: Asymmetry* **2006**, *17*, 687.
29. Sanfilippo, C.; D'Antona, N.; Nicolosi, G. *Tetrahedron: Asymmetry* **2006**, *17*, 12.
30. Chelucci, G.; Baldino, S.; Pinna, G. A.; Benaglia, M.; Buffa, L.; Guizzetti, S. *Tetrahedron* **2008**, *64*, 7574.
31. Toda, F.; Mori, K.; Stein, Z.; Goldberg, I. *Tetrahedron Lett.* **1989**, *30*, 1841.
32. Nakajima, M.; Sasaki, Y.; Shiro, M.; Hashimoto, S. *Tetrahedron: Asymmetry* **1997**, *8*, 341.
33. Clayden, J.; Fletcher, S. P.; McDouall, J. J. W.; Rowbottom, S. J. M. *J. Am. Chem. Soc.* **2009**, *131*, 5331.
34. Freedman, T. B.; Cao, X.; Dukor, R. K.; Nafie, L. A. *Chirality* **2003**, *15*, 743.
35. Stephens, P. J.; Devlin, F. J.; Pan, J. J. *Chirality* **2008**, *20*, 643.
36. Uncuta, C.; Ion, S.; Gherase, D.; Bartha, E.; Teodorescu, F.; Filip, P. I. *Rev. Chim.* **2009**, 86.
37. Teodorescu, F.; Naubron, J.-V.; Uncuța, C.; Filip, P. I.; Bartha, E.; Toader, A. M.; Man, I. C. *Tetrahedron: Asymmetry* **2014**, *25*, 725.
38. Polavarapu, P. L. *Chirality* **2008**, *20*, 664.
39. Paun, I. Ph.D., 'C.D. Nenitzescu' Institute of Organic Chemistry, Bucharest and Université Aix-Marseille III, Faculté des Sciences et des Techniques de Saint-Jêrome, Marseille, 1995.
40. Uncuta, C.; Caproiu, M. T.; Campeanu, V.; Petride, A.; Danila, M. G.; Plaveti, M.; Balaban, A. T. *Tetrahedron* **1998**, *54*, 9747.
41. Balaban, T. S.; Balaban, A. T. *'Pyrilium salts', Science of Synthesis, Houben-Weyl Methods of Molecular Transformations*; Georg Thieme: Stutgart, 2003.
42. Frisch, M. J.; Trucks, G. W.; Schlegel, H. B.; Scuseria, G. E.; Robb, M. A.; Cheeseman, J. R.; Scalmani, G.; Barone, V.; Mennucci, B.; Petersson, G. A.; Nakatsuji, H.; Caricato, M.; Li, X.; Hratchian, H. P.; Izmaylov, A. F.; Bloino, J.; Zheng, G.; Sonnenberg, J. L.; Hada, M.; Ehara, M.; Toyota, K.; Fukuda, R.; Hasegawa, J.; Ishida, M.; Nakajima, T.; Honda, Y.; Kitao, O.; Nakai, H.; Vreven, T., ; Montgomery, J. A., Jr.; Peralta, J. E.; Ogliaro, F.; Bearpark, M.; Heyd, J. J.; Brothers, E.; Kudin, K. N.; Staroverov, V. N.; Kobayashi, R.; Normand, J.; Raghavachari, K.; Rendell, A.; Burant, J. C.; Iyengar, S. S.; Tomasi, J.; Cossi, M.; Rega, N.; Millam, J. M.; Klene, M.; Knox, J. E.; Cross, J. B.; Bakken, V.; Adamo, C.; Jaramillo, J.; Gomperts, R.; Stratmann, R. E.; Yazyev, O.; Austin, A. J.; Cammi, R.; Pomelli, C.; Ochterski, J. W.; Martin, R. L.; Morokuma, K.; Zakrzewski, V. G.; Voth, G. A.; Salvador, P.; Dannenberg, J. J.; Dapprich, S.; Daniels, A. D.; Farkas, Ö.; Foresman, J. B.; Ortiz, J. V.; Cioslowski, J.; Fox, D. J. *Gaussian09; Revision A2*; Gaussian: Wallingford CT, 2009.
43. Stephens, P. J.; Harada, N. *Chirality* **2010**, *22*, 229.